J Intell Robot Syst (2017) 85:331–352
DOI 10.1007/s10846-016-0401-9

Identification-Based Robust Motion Control of an AUV: Optimized by Particle Swarm Optimization Algorithm

Sayed Hamid Mousavian · Hamid Reza Koofigar

Received: 3 November 2014 / Accepted: 4 July 2016 / Published online: 18 July 2016

Abstract In this paper, the problem of identification-based robust motion control of an Autonomous Underwater Vehicle (AUV) is investigated. The unknown system parameters are estimated by using an adaptive parameter identifier, whose gains are optimized by Particle Swarm Optimization (PSO) algorithm. Removing the trial and error procedure and ensuring the convergence property together with fast response, are the benefits of such identification scheme. On the other hand, the system uncertainties, hydrodynamic parameter variations and external disturbances which affect the identified dynamical model, are also taken into account. The cross-coupling effects between subsystems are also considered as model uncertainties. Such uncertain model is then adopted in control synthesis procedure, in the steering and diving modes. In order to achieve the robust stability and performance, two robust control strategies are presented here to solve the motion control problem. First, an H_∞ mixed sensitivity problem is formulated in which the weighting functions are selected based on an optimization criterion, by using PSO algorithm. Controller order reduction is also applied to the resulting diving and steering controllers, using the Hankel norm approximation. Then, an Adaptive Sliding Mode Control (ASMC), whose sliding surface coefficients are optimized by PSO algorithm, is developed for the identified AUV model. Possessing the robustness properties with respect to system perturbations, the developed Sliding Mode Control (SMC) removes the complexity of uncertain model representation and the limitations on choosing the weighting functions in the H_∞ control problem. The upper bounds of perturbations are not required to be known in the proposed control schemes. The simulation results are also presented to demonstrate the performance of the proposed identification-based control methods.

Keywords Autonomous underwater vehicle · Robust control · Adaptive identification · Model uncertainty · PSO algorithm

S. H. Mousavian · H. R. Koofigar (✉)
Department of Electrical Engineering, University of Isfahan, Isfahan 8174673441, Iran
e-mail: koofigar@eng.ui.ac.ir

S. H. Mousavian
e-mail: H.mousavian@eng.ui.ac.ir

1 Introduction

Motion control of underwater vehicles is one of the main topics in oceanic research and engineering, as AUVs play an important role in deep-water missions, oil and gas extraction and exploration [1], commercial and scientific missions [2], and geological and biological investigations [3, 4]. Controller design for an AUV is a challenging problem, due to some reasons as

1) Non-linear dynamics of the vehicle subject to hydrodynamic forces and moments.

2) Model uncertainties, due to unmodelled dynamics and poor knowledge of hydrodynamic and damping coefficients.
3) External disturbances such as underwater currents.

The performance of model-based control algorithms depends mainly on the precision of system modeling and the accuracy of the model parameters. Although a six degree-of-freedom (DOF) model is commonly used to describe the nominal behavior of AUVs, but from a practical viewpoint, various kinds of uncertainties and disturbances may perturb the system and form an uncertain nonlinear model. In the most of applications, parameter variations and environmental disturbances make the motion deviate from the desired trajectory [5].

As a preliminary step to control design procedure, various investigations have been devoted to identify the dynamical model of AUVs, such as least square method [6], extended Kalman filter [7, 8], maximum likelihood method [8], and adaptive identification technique [9]. Such algorithms, committed to approximating the hydrodynamic parameters in the mathematical model, suffer from some restrictions as dependency to the initial conditions, ill-conditioned solutions and simultaneous drift. Removing such drawbacks, some novel algorithms, e.g. neural networks [10] and neurofuzzy [11], are proposed to identify the hydrodynamic parameters in some special classes of AUVs. However, the nonlinearities and coupled terms make the identification of the whole hydrodynamic coefficients quite complicated and time consuming. Thus, the general structure of AUV model usually needs to be simplified prior to the identification process. A set of decoupled AUV subsystems, concerning with different degrees of freedom can be set up based on Kalman filter identification [12]. Furthermore, adaptive parameter identifiers may be also adopted to obtain the linear model of decoupled AUV subsystems [13], in which the adaptation gains have an important role in the speed of convergence. Some metaheuristic or evolutionary algorithms may be used to remove the trial and error procedure for gain selection. To this end, the PSO algorithm as an intelligent optimization technique, is used here to optimally determine the adaptation gains Compared with some other naturally inspired methods, such as genetic algorithm, the PSO technique gives faster convergence with a few parameters to be adjusted. In addition, unlike the heuristic methods as simulated annealing and evolutionary algorithms, the PSO includes a flexible and well-balanced mechanism to enhance the global and local exploration with a rather short processing time.

During the past years, complete, decoupled, and linearized models of AUVs have been used to design motion control algorithms. Adopting the linearized dynamics, various linear control techniques such as PID controller [14], LQR and LQG algorithms [14, 15] have been developed. Some more recent investigations have decoupled the diving plane and steering system states [13, 16], to develop the depth, pitch, and yaw controllers [17, 18]. By taking the complete model, some six DOF controllers, based on adaptive identification and intelligent algorithms, have been reported to achieve the desired performance [19, 20]. The previous works suffer from at least one of the following restrictions, (i) the conservative assumptions make the algorithm be applicable for a special class of AUVs, (ii) unmodelled dynamics, parameter variations and environmental disturbances are not incorporated in dynamical equations altogether, (iii) robust closed-loop stability and performance are not ensured analytically.

Concerning with robust motion control of AUVs, H_∞ control strategy may take the unstructured uncertainties into account, to guarantee the desired stability and performance. Robust stability, fast tracking response and disturbance attenuation can be well suited in an H_∞ design framework. In fact, the control problem is expressed as a mathematical optimization problem whose solution minimizes the H_∞ norm of the closed-loop transfer function and internally stabilizes the system. Weighting function selection and high order of the resulting controller may be the main problems in developing an H_∞ control algorithm [21]. The weighting functions have no general structure and should be assigned in each specific design. The SMC, as a less conservative nonlinear robust control technique, is then adopted to solve the underlying control problem [22]. Selection of the sliding surface and its coefficients are usually the main issues of the SMC, as the closed loop performance and transient response are affected by such selections.

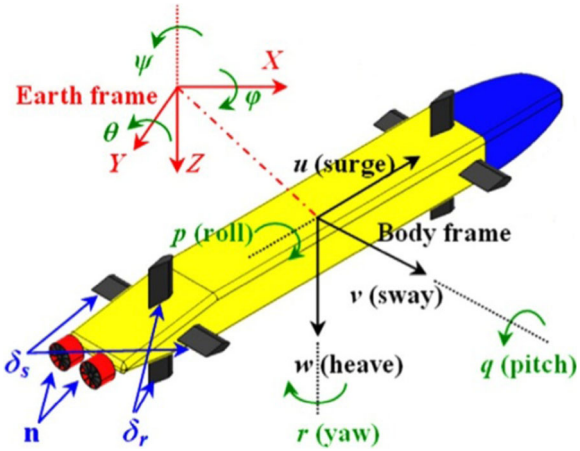

Fig. 1 Coordinate systems for an AUV [23]

In general, the benefits of the proposed techniques for identification and motion control of an AUV, compared with some previous works, can be stated as

1) An optimal performance is obtained by selecting the coefficients of weighting functions, the sliding surface and adaptation gains, by using the PSO algorithm.
2) The coupling effects, as model uncertainties, may be compensated in robust motion control.
3) No prior knowledge about the upper bound of perturbations is required in control design.
4) The chattering phenomenon of the conventional SMC is removed here by the proposed PSO-based ASMC.
5) Simple structure of the identification mechanism and control laws may provide easy real-time implementation with low computations

The remainder of this paper is organized as follows. Introducing the nonlinear equations of motion, the steering and diving subsystems are decomposed in Section 2. The PSO-based adaptive identification algorithm is constructed in Section 3 to optimally determine the unknown parameters of the AUV model. Adopting the identified model, two robust motion control algorithms are developed based on the H_∞ control scheme and sliding mode strategy in Section 4. From a comparison point of view, the effectiveness of the developed algorithms is discussed by giving various simulation results in Section 5. The concluding remarks are finally given in Section 6.

2 Dynamic Motion Equations of AUV

The dynamic model of an underwater vehicle can be developed through the Newton-Euler formulation. The motion of an AUV in a three-dimensional space may be analyzed by defining a frame, including the position and orientation of the rigid body. In general, the AUV model may be written either in a body-fixed frame, as in this work, or in an earth-fixed (inertial) coordinate, as demonstrated in Fig. 1.

2.1 General Mathematical Model Structure

The nonlinear dynamic equations of motion for a 6-DOF AUV can be written in the body-fixed frame as [14]

$$M(v)\dot{v} + C(v)v + D(v)v + g(\eta) = \tau + \tau_D \tag{1}$$

$$\dot{\eta} = J(\eta)v \tag{2}$$

where $v = [u\ v\ w\ p\ q\ r]^T$ is the AUV spatial velocity state vector, and $\eta = [x\ y\ z\ \phi\ \theta\ \psi]^T$ includes the position and orientation states, as introduced in Table 1. The spatial transformation matrix between

Table 1 Notation used for marine vehicle

DOF	Motion descriptions	Positions and orientations	Linear and angular velocities	Forces and moments
1	Motion in the x-direction (Surge)	x	u	X
2	Motion in the$y$-direction (Sway)	y	v	Y
3	Motion in the$z$-direction (Heave)	z	w	Z
4	Rotations about the$x$-axis (Roll)	ϕ	p	K
5	Rotations about the$y$-axis (Pitch)	θ	q	M
6	Rotations about the$z$-axis (Yaw)	ψ	r	N

the inertial frame and the body-fixed frame is denoted by $J(\eta)$. Moreover, $M(\upsilon)$ is the inertia matrix, $C(\upsilon)$ is the matrix of centrifugal and Coriolis terms, due to the rigid body and the added mass, $D(\upsilon)$ is a diagonal matrix of damping or drag terms, and $g(\eta)$ represents the vector of gravity and buoyancy forces and moments. The control forces and moments are included in $\tau = [X\ Y\ Z\ K\ M\ N]^T$, and τ_D is the vector of external disturbances.

2.2 Model Decomposition for AUV

Based on the rigid-body motion principle, a 6-DOF model of AUV can be decomposed into three non-interaction subsystems control, as [14]

1) Steering subsystem, used to control the yaw (heading) angle ψ by using the rudder angle δ_r as the control input variable.
2) Diving subsystem, to control the depth z and pitch angle θ by the elevator (stern plane) angle δ_s as the control input variable.
3) Speed subsystem (surge velocity), to control the vehicle speed by varying the propeller speed.

In practice, the surge speed is constant and only the steering and diving subsystems should be taken in designing the identification-based motion controllers.

2.2.1 Steering Mode

Neglecting the motion of vehicle in the vertical plane, the heading direction may be controlled by the rudder angle. In the steering mode, a linear model is obtained for the vehicle as [14]

$$\begin{bmatrix} m - Y_{\dot{v}} & mx_G - Y_{\dot{r}} & 0 \\ mx_G - N_{\dot{v}} & I_Z - N_{\dot{r}} & 0 \\ 0 & 0 & 1 \end{bmatrix} \begin{bmatrix} \dot{v} \\ \dot{r} \\ \dot{\psi} \end{bmatrix} + \begin{bmatrix} -Y_v & mu_0 - Y_r & 0 \\ -N_v & mx_G u_0 - N_r & 0 \\ 0 & -1 & 0 \end{bmatrix} \begin{bmatrix} v \\ r \\ \psi \end{bmatrix} = \begin{bmatrix} Y_{\delta_r} \\ N_{\delta_r} \\ 0 \end{bmatrix} \quad (3)$$

where m, I_z, u_0 and x_G respectively are the mass of the vehicle, the vehicle inertia around the yaw axis, the surge velocity and the position of the center of gravity. The other parameters are the hydrodynamic parameters including the cross-flow drag coefficients ($Y_v Y_r N_v N_r$), the added mass coefficients ($Y_{\dot{v}} Y_{\dot{r}} N_{\dot{v}} N_{\dot{r}}$), the fin lift force ($Y_{\delta_r}$) and moment ($N_{\delta_r}$) [14].

2.2.2 Diving Mode

For a vehicle in the vertical plane, it is assumed that the forward speed is constant, the heave velocity is small and $x_G = 0$. This is quite realistic, as the most of small underwater vehicles move slowly in the vertical direction. Thus, the vehicle can be modeled in this mode by a linear form as [14]

$$\begin{bmatrix} \dot{q} \\ \dot{\theta} \\ \dot{z} \end{bmatrix} = \begin{bmatrix} \frac{M_q}{I_y - M_{\dot{q}}} & -\frac{(z_G - z_B)W}{I_y - M_{\dot{q}}} & 0 \\ 1 & 0 & 0 \\ 0 & -u_0 & 0 \end{bmatrix} \begin{bmatrix} q \\ \theta \\ z \end{bmatrix} + \begin{bmatrix} \frac{M_{\delta_r}}{I_y - M_{\dot{q}}} \\ 0 \\ 0 \end{bmatrix} \delta_s \quad (4)$$

where I_y, u_0, W and $(z_G - z_B)$ respectively are the vehicle inertia around the pitch axis, the surge velocity the weight of the vehicle and the distance between the gravity and the body center. The remainder of parameters are the hydrodynamic parameters, including the cross-flow drag coefficient (M_q), the added mass coefficient ($M_{\dot{q}}$) and the fin lift moment (M_{δ_s}) [14].

3 PSO-Based Adaptive Identification

Various system identification techniques, classified to parametric and nonparametric techniques have been successfully applied for the vehicle model identification. The parametric approaches commonly adopt a mathematical structure whose unknown parameters are estimated. Adaptive identification as a parametric scheme, is used here to identify the unknown matrices of the model in the steering and diving modes. Furthermore, the PSO algorithm can be used to improve the design specifications.

3.1 Overview of Particle Swarm Optimization

The particle swarm optimization approach, as a population-based stochastic searching technique, was proposed by Kennedy and Eberhart in 1995 [24]. Each individual (named particle) of the population (called swarm), adjusts its trajectory towards its own previous best solution and the previous best solution attained by any particle of its topological neighborhood. The particles in PSO are specified by two main characteristics, including the position and velocity. The

current position and velocity vector of the ith particle in the search space are respectively denoted by $X_i = (x_{i1}, x_{i2}, ..., x_{id})$ and $V_i = (v_{i1}, v_{i2}, ..., v_{id})$. The best earlier position of the ith particle is represented by $Pbest_i = (pbest_{i1}, pbest_{i2}, ..., pbest_{id})$ and the global best position in the swarm, up to iteration k, is called $Gbest^k$.

The PSO update formula is given by

$$V_i^{k+1} = w_I V_i^k + c_1 r_1 (Pbest_i^k - X_i^k) + c_2 r_2 (Gbest^k - X_i^k) \quad (5)$$

$$X_i^{k+1} = X_i^k + V_i^{k+1} \Delta t \quad (6)$$

where c_1 (cognitive parameter) and c_2 (social parameter) are two positive constants, r_1 and r_2 are two random functions in [0 1], Δt is time increment in discretization, w_I is the inertia weight and k is the pointer of iterations (generations), which plays an important role in convergence behavior. Due to the importance of the inertia weight in handling the global/local search behavior of the PSO algorithm, a dynamic improvement has been proven to be useful by decreasing the inertia weight, based on a fraction multiplier k_w ($0 < k_w < 1$) as [26]

$$w_I^{k+1} = k_w w_I^k \quad (7)$$

In fact, PSO algorithm performs faster in finding solutions, compared with some other evolutionary computation techniques [25]. Some reasons for such property, can be stated as [24–26]

1) In PSO, the momentum effects on particle movement can allow faster convergence (e.g. when a particle is moving in the direction of a gradient) with more variety/diversity in search trajectories.
2) PSO does not need reproduction or mutation to produce the next generation. Instead, the particles, as the potential solutions, fly through the problem space by following the current optimum particles. Meanwhile, all of particles share the obtained information, and such interactive behavior makes the search efficient.
3) In some techniques, e.g. genetic algorithm the whole population moves like one group towards an optimal area, while in PSO each particle commonly tends to converge to the best solution.
4) In PSO, the particles update themselves with the internal velocity. They also have memory, as an important tool in finding the solutions fast.

3.2 Adaptive Model Parameter Identifier Optimized by PSO

In order to use an identification algorithm the steering and diving subsystems may be represented in a state space form, by ignoring the index of subsystems symbols, as

$$\dot{x} = A_p x + B_p u \quad (8)$$

in which A_p is stable, u is a bounded input. To estimate A_p and B_p, the so-called series-parallel model may be introduced by [13]

$$\dot{\hat{x}} = A_m \hat{x} + (\hat{A}_p - A_m) x + \hat{B}_p u \quad (9)$$

where A_m is an arbitrary stable matrix, $\hat{x}$ is the estimate of x and $\hat{A}_p$ and $\hat{B}_p$ denote the estimates of A_p and B_p respectively.

By defining the estimation error $\epsilon = x - \hat{x}$, one can derive the adaption mechanisms

$$\dot{\hat{A}}_p = \gamma_A \in x^T \quad (10)$$

$$\dot{\hat{B}}_p = \gamma_B \in u^T \quad (11)$$

where $\gamma_A, \gamma_B > 0$ are the adaption gains [13].

The convergence of $\hat{A}_p$ and $\hat{B}_p$ to their true values A_p and B_p, depends on the properties of the input u. More precisely, if u belongs to the class of sufficiently rich inputs, i.e., u has enough frequencies to excite all the modes of the plant, then the vector $\left[x^T, u^T\right]^T$ has the Persistent Excitation (PE) property and the exponentially fast convergence is guaranteed [13].

The parametric structures of the steering subsystem (3) and diving subsystem (4) are specified respectively by

$$A_{p\_S} = \begin{bmatrix} a_{11\_S} & a_{12\_S} & 0 \\ a_{21\_S} & a_{22\_S} & 0 \\ 0 & 1 & 0 \end{bmatrix},$$

$$B_{p\_S} = \begin{bmatrix} b_{1\_S} \\ b_{2\_S} \\ 0 \end{bmatrix},$$

$$x_S = [v\ r\ \psi]^T\ ,\ u_S = \delta_r\ ,\ y_S = \psi \quad (12)$$

$$A_{p\_D} = \begin{bmatrix} a_{11\_D} & a_{12\_D} & 0 \\ 1 & 0 & 0 \\ 0 & -u_0 & 0 \end{bmatrix},$$

$$B_{p\_D} = \begin{bmatrix} b_{1\_D} \\ 0 \\ 0 \end{bmatrix},$$

$$x_D = [q\ \theta\ z]^T\ , u_D = \delta_s\ , y_D = z \tag{13}$$

where the surge velocity is constant as $u_0 = 1.832 m/sec$ [22]. In this study, to identify the steering and diving modes, the input is chosen sufficiently rich respectively of orders 6 and 4 as

$$u_{i\_S}(t) = 5\ \sin t + 5\ \sin 4t + \sin 8t \tag{14}$$

$$u_{i\_D}(t) = 10\ \sin 16t + 5\ \sin 4t \tag{15}$$

Remark 1 There is a trade off in choosing γ_A and γ_B to obtain the fast convergence and avoiding instability. Compared with some previous conventional works [9, 13], the adaptation gains is determined here by PSO to achieve the fast convergence and avoid the windup problem simultaneously. This advantage is significant, especially for uncertain systems. The proposed block diagram of the parameter identification scheme, tuned by PSO is presented in Fig. 2.

The cost function, used in PSO is adopted here as

$$h_{Total}(\gamma_A, \gamma_B) = \int_{t=0}^{T_f} (|e_1(t)| + |e_2(t)| + |e_3(t)|)\ dt \tag{16}$$

where $e_i(t) = x_i(t) - \hat{x}_i(t)$, $i = 1, 2, 3$ and $T_f > 0$ is the final simulation time.

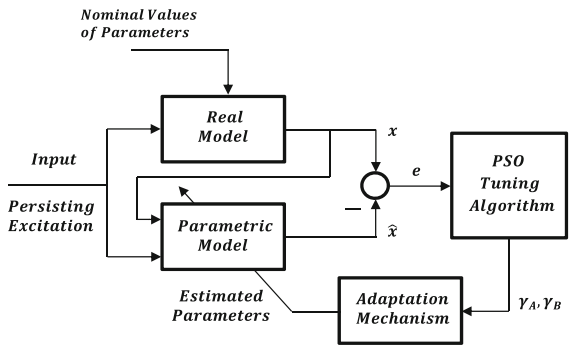

Fig. 2 The proposed block diagram of model parameter identification tuned by PSO

By Eqs. 8–13, the adaptation mechanisms for the steering and diving modes are obtained as

$$\begin{aligned} \dot{\hat{a}}_{11\_S} &= \gamma_{A\_11\_S}\left(x_1 - \hat{x}_1\right) x_1\ , \\ \dot{\hat{a}}_{12\_S} &= \gamma_{A\_12\_S}\left(x_1 - \hat{x}_1\right) x_2\ , \\ \dot{\hat{b}}_{2\_1\_S} &= \gamma_{B\_1\_S}\left(x_1 - \hat{x}_1\right) u_{i\_S} \end{aligned} \tag{17}$$

$$\begin{aligned} \dot{\hat{a}}_{21\_S} &= \gamma_{A\_21\_S}\left(x_2 - \hat{x}_2\right) x_1\ , \\ \dot{\hat{a}}_{22\_S} &= \gamma_{A\_22\_S}\left(x_2 - \hat{x}_2\right) x_2\ , \\ \dot{\hat{b}}_{2\_2\_S} &= \gamma_{B\_2\_S}\left(x_2 - \hat{x}_2\right) u_{i\_S} \end{aligned} \tag{18}$$

and

$$\begin{aligned} \dot{\hat{a}}_{11\_D} &= \gamma_{A\_11\_D}\left(x_1 - \hat{x}_1\right) x_1\ , \\ \dot{\hat{a}}_{12\_D} &= \gamma_{A\_12\_D}\left(x_1 - \hat{x}_1\right) x_2\ , \\ \dot{\hat{b}}_{1\_D} &= \gamma_{B\_1\_D}\left(x_1 - \hat{x}_1\right) u_{i\_D} \end{aligned} \tag{19}$$

where $\gamma_{A\_S}, \gamma_{B\_S}, \gamma_{A\_D}, \gamma_{B\_D}$ are some constants determined by using PSO with the specified cost function.

Based on the proposed block diagram in Fig. 2, the PSO-based identification problem is to find the optimal vectors

$$\gamma_{\_S} = [\gamma_{A\_11\_S}\ ,\ \gamma_{A\_12\_S}\ ,\ \gamma_{B\_1\_S}\ ,\ \gamma_{A\_21\_S}\ ,\ \gamma_{A\_22\_S}\ ,\ \gamma_{B\_2\_S}] \tag{20}$$

and

$$\gamma_{\_D} = [\gamma_{A\_11\_D}\ ,\ \gamma_{A\_12\_D}\ ,\ \gamma_{B\_1\_D}] \tag{21}$$

that minimizes the objective function $h_{Total}(\gamma_A, \gamma_B)$, in the steering and diving modes respectively.

The specifications of the applied PSO algorithm, used for identification of the steering and diving modes, are summarized in Table 2. The specified inputs (14) and (15) are used in adaptation mechanisms (17)–(19), based on Fig. 2. Then, the PSO algorithm is applied to find the optimal values of the parameters of $\gamma_{\_S}$ and $\gamma_{\_D}$, by minimizing the objective function $h_{Total}(\gamma_A, \gamma_B)$ in (16). The adopted lower and upper bounds of nine parameters in $\gamma_{\_S}$ and $\gamma_{\_D}$ and the final optimal values for adaptation gains in (20) and (21) are given in Table 3. Now, by replacing the optimal vectors $\gamma_{\_S} = [9\ ,\ 8\ ,\ 0.3\ ,\ 9\ ,\ 19\ ,\ 0.8]$ and $\gamma_{\_D} = [15.1\ ,\ 9.98\ ,\ 1.01]$ in Eqs. (17)–(19), the unknown parameters of matrices in (12) and (13) can be estimated.

Figures 3 and 4 demonstrate the time history of parameter identification in the steering and diving modes, respectively. Moreover, the estimated values of

Table 2 The steps of PSO algorithm in the identification problem

Step	Process
1	Set the members of each individual in PSO algorithm $\gamma_{\_S}$ and $\gamma_{\_D}$
2	Population size is equal to 50
3	Inertia weight factor w_I is set as Eq. 7, with $w_I(0) = 0.975$
4	The limit of change in velocity is set to maximum dynamic range of the variables on each dimension
5	Acceleration constants are $c_1 = c_2 = 2.05$
6	Maximum iteration is set to 20

the unknown parameters in steady state are reported in Table 4. By replacing the estimated parameters in (12) and (13), the transfer function (nominal plant) for the steering and diving modes are respectively obtained as

$$G_{n\_S}(s) = \frac{\psi(s)}{\delta_r(s)} = \frac{-0.2847\,s - 0.08408}{s^3 + 0.8457\,s^2 + 0.1205\,s} \tag{22}$$

and

$$G_{n\_D}(s) = \frac{z(s)}{\delta_s(s)} = \frac{0.382}{s^3 + 0.9999\,s^2 + 0.0665\,s} \tag{23}$$

4 Robust Motion Control Design

Adopting the identified model of AUV in Section 3, and taking the model uncertainties into account, an H_∞ mixed sensitivity problem is first formulated to meet reference tracking, disturbance attenuation and avoiding actuator saturation. Besides, to remove the restriction of weighting function selection, the PSO algorithm is adopted to optimally determine the coefficients of the prescribed weighting functions. Then, from a comparison viewpoint sliding mode control is also formulated to solve the underlying problem.

4.1 H_∞ Control Formulation

Unstructured uncertainties arise mostly due to modeling errors and linearization, may be tackled by H_∞ control. To this end, a family of unknown plants is first constructed based on the nominal model. The input multiplicative uncertainty is preferred here to describe the steering and diving subsystems as

$$G_p(s) = G_n(s)\,(1 + \Delta_m(s)\;W_{\mathrm{m}}(s)) \tag{24}$$

where G_n denotes the nominal system, $W_{\mathrm{m}}(s)$ is a stable weighting function and $\Delta_m(s)$ indicates the normalized uncertainty block with $\|\Delta_m(s)\|_\infty < 1$ [27, 28], which together with Eq. 24 yields

$$\left|\frac{G_p(j\omega)}{G_n(j\omega)} - 1\right| \le |W_{\mathrm{m}}(j\omega)| \qquad \forall\omega \tag{25}$$

where $|W_{\mathrm{m}}(j\omega)|$ represents the upper bound of uncertainty in frequency domain.

Now, a mixed sensitivity problem can be formulated to solve the control problem, as demonstrated in Fig. 5. To facilitate the designing procedure, a general

Table 3 The optimal values of γ_{A_S}, γ_{B_S}, γ_{A_D}, γ_{B_D} in the steering and diving modes

Subsystem							
Steering mode	Parameters	$\gamma_{A\_11\_S}$	$\gamma_{A\_12\_S}$	$\gamma_{A\_21\_S}$	$\gamma_{A\_22\_S}$	$\gamma_{B\_1\_S}$	$\gamma_{B\_2\_S}$
	Lower Bound	7	7	0.15	7	12	0.5
	Upper Bound	14	14	0.3	14	24	1
	Optimal Value	9	8	0.3	9	19	0.8
Diving mode	Parameters	$\gamma_{A\_11\_D}$	$\gamma_{A\_12\_D}$	$\gamma_{B\_1\_D}$			
	Lower Bound	10	9	0.6			
	Upper Bound	20	18	1.2			
	Optimal Value	15.1	9.98	1.01			

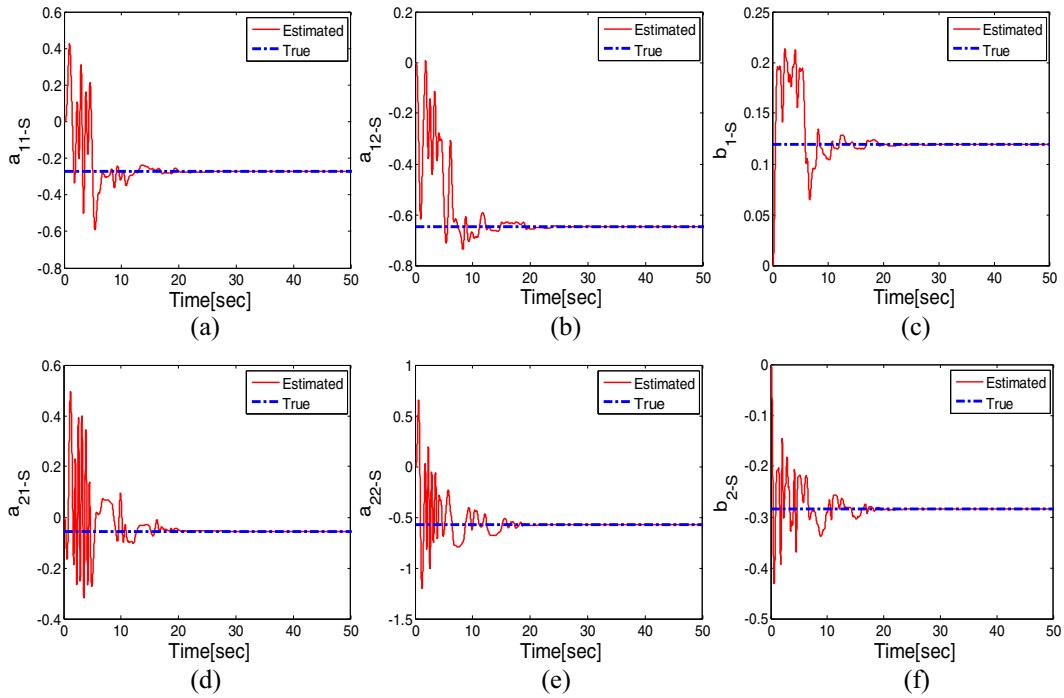

Fig. 3 Time history of parameter estimation in the steering mode (**a**) a_{11_S}, (**b**) a_{12_S}, (**c**) b_{1_S}, (**d**) a_{21_S}, (**e**) a_{22_S} , (**f**) b_{2_S}

framework is formed by the linear fractional transformation, as depicted in Fig. 6. By defining $Z = \begin{bmatrix} z_1 & z_2 \end{bmatrix}^T$ and $w = d$, respectively as the controlled output and the exogenous input, the generalized plant $\boldsymbol{P}$ is specified as

$$\begin{bmatrix} y_\Delta \\ z_1 \\ z_2 \\ y \end{bmatrix} = \underbrace{\begin{bmatrix} 0 & 0 & W_m \\ -\mathrm{G}_n W_e & -W_e & -\mathrm{G}_n W_e \\ 0 & 0 & W_u \\ -\mathrm{G}_n & -1 & -\mathrm{G}_n \end{bmatrix}}_{\boldsymbol{P}} \begin{bmatrix} u_\Delta \\ d \\ u \end{bmatrix} \tag{26}$$

The H_∞ controller K_{inf} is designed so that y_m tracks the reference trajectory y_d, taking the effects of disturbance and the actuator limit, into account. The sensitivity-performance weighting function W_e, is selected such that the performance requirements on rise time, overshoot percentage and steady state error are satisfied. Meanwhile, the transfer function W_u, penalizes the controller with high control effort.

Briefly discussing, the purpose of the underlying mixed-sensitivity problem is to minimize a cost function, including the transfer functions

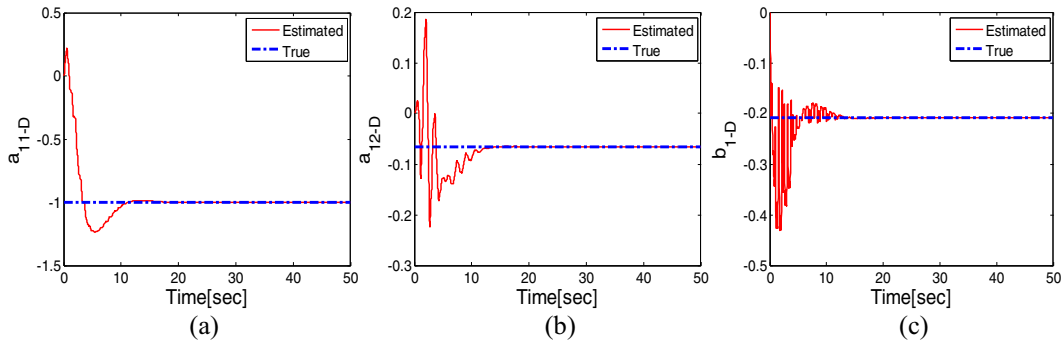

Fig. 4 Time history of parameter estimation in diving plane (**a**) a_{11_D}, (**b**) a_{12_D}, (**c**) b_{1_D}

Table 4 Estimated values of unknown parameters in steering and diving modes

Subsystem							
Steering mode	Parameters	a_{11_S}	a_{12_S}	a_{21_S}	a_{22_S}	b_{1_S}	b_{2_S}
	Estimated Value	−0.2721	−0.6465	−0.0552	−0.5734	0.1191	−0.2848
Diving mode	Parameters	a_{11_D}	a_{12_D}	b_{1_D}			
	Estimated Value	−1	−0.0665	−0.2085			

i. From u_Δ to y_Δ (robust stability)
ii. From external disturbance d to system output y_m (disturbance attenuation)
iii. From the reference input y_d to controller output u (avoiding actuator saturation)

Defining the sensitivity function $S = \left(1 + \mathrm{G}_n\, K_{inf}\right)^{-1}$, the norm of transfer matrix T_{zw} is given by

$$\|T_{zw}\|_\infty = \left\| \begin{array}{c} W_m G_n K_{inf}\, S \\ W_e\, S \\ W_u K_{inf}\, S \end{array} \right\|_\infty \tag{27}$$

The H_∞ sub-optimal control uses the γ-iteration algorithm to give an infimum value for $\gamma > 0$ such that the objectives are satisfied and $\|T_{zw}\|_\infty < \gamma$ [21]. On the other hand, the calculated value of γ is highly dependent to the selected weighting functions. Hence, some general guidelines are presented on choosing the structure of such functions and using the PSO algorithm to optimally determine the coefficients.

4.1.1 Weighting Functions Selection

To determine the uncertainty function Δ for each subsystem, based on the specified procedure in [28, 29, 31] the transfer functions (22) and (23) are first adopted as the nominal model $G_n\,(j\omega)$ in Eq. 24 for the steering and diving subsystems. Then, various parameters of the model for the worst case configuration are perturbed up to ±40% of their nominal values.

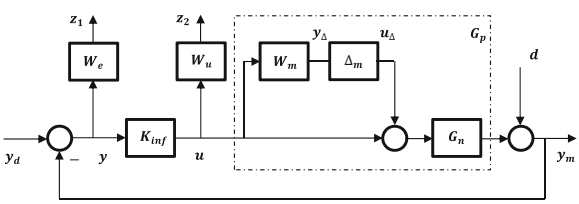

Fig. 5 Block diagram representation of the system with multiplicative uncertainty

The singular values of the perturbed system $G_p\,(j\omega)$, together with the specified multiplicative weighting functions $W_{\mathrm{m}}\,(j\omega)$ are plotted in Fig. 7.

The input multiplicative uncertainty weighting functions are approximated by a first order system and tuned to get the best possible match for the steering mode as

$$W_{\mathrm{m\_S}}(s) = \frac{0.5774\, s + 2.257}{s + 3.091} \tag{28}$$

and for diving plane as

$$W_{\mathrm{m\_D}}(s) = \frac{0.5834\, s + 2.137}{s + 2.252} \tag{29}$$

A similar procedure can be carried out to optimally determine W_e and W_u in the steering and diving modes. A general structure for such weightings may be a first order transfer function [21] respectively as

$$W_e(s) = \frac{A\, s + B}{s + C} \tag{30}$$

and

$$W_u(s) = \frac{s + D}{E\, s + F} \tag{31}$$

where A, B, C, D, $E$and F are some constants, determined by using the PSO algorithm. The weighting function W_e is selected such that $|W_e\,(j\omega)|^{-1} \geq |S\,(j\omega)|\,, \forall\omega$, i.e. the tracking performance and disturbance attenuation are satisfied and W_u should satisfy $|W_u\,(j\omega)|^{-1} \geq \left|K_{inf}\,(j\omega)\; S\,(j\omega)\right|\,, \forall\omega$, by

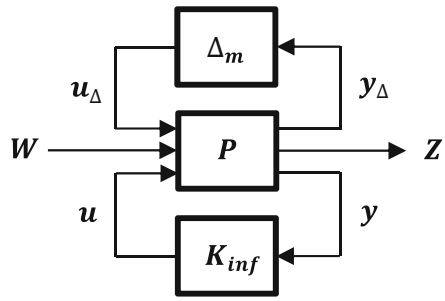

Fig. 6 General framework for H_∞ controller design

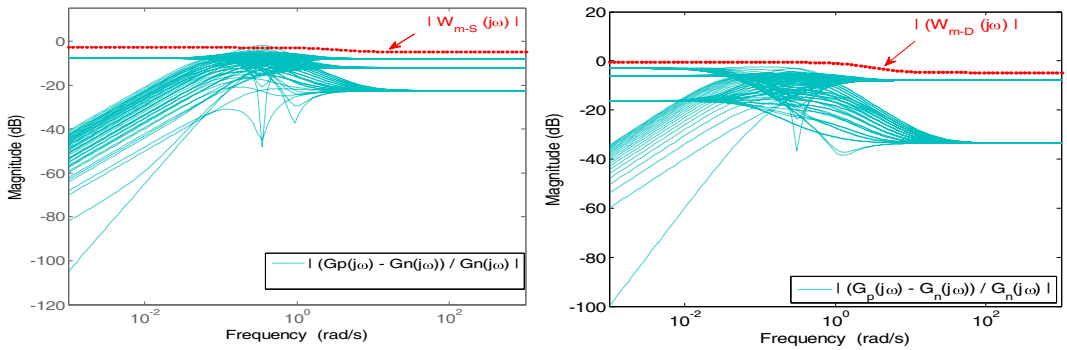

Fig. 7 The singular values of the perturbed system in (**a**) steering mode and (**b**) diving mode

which the maximum amplitude of control effort can be taken into account [21]. Also, defining the complementary sensitivity function $T(j\omega) = G_n(j\omega) K_{inf}(j\omega) S(j\omega)$, the inequality condition $|W_m(j\omega)|^{-1} \geq |T(j\omega)|, \forall\omega$, may be adopted together with inequality (25) to ensure the robust stability, in choosing W_m.

Now, the PSO algorithm can be used to optimally determine the unknown vector

$$\lambda = [A, B, C, D, E, F] \tag{32}$$

by specifying a performance index. Including overshoot percentage M_P, rise time t_r, and settling time t_s in the step response of the closed loop syste, a weighted cost function is chosen as

$$J_1(\lambda) = w_1 M_P + w_2 t_r + w_3 t_s \tag{33}$$

in which the weight factors w_i, $i = 1, 2, 3$ are specified by the designer. On the other hand, the weighting functions inevitably affect the value of γ in the suboptimal H_∞ algorithm. Hence, a second index may be also imposed by

$$J_2(\lambda) = \|T_{zw}\|_\infty \tag{34}$$

incorporated in forming the total objectives function

$$J_{Total}(\lambda) = J_1(\lambda) + J_2(\lambda) \tag{35}$$

The resulting PSO-based weighting function selection is to find λ, so that the cost function (35) is minimized, based on the proposed block diagram in Fig. 8.

The lower bound of thesix parameters in vector λ is taken to zero and the upper bounds are assumed to be $[A, B, C, D, E, F] = [0.005, 0.5, 30, 25, 25, 1000]$, in the PSO algorithm simulation. The weight factors in Eq. 33 are selected as $w_1 = w_2 = 50$ and $w_3 = 20$, to get the fast responses with low overshoot percentage. Finally, by replacing the obtained optimal values of the entries of λ in general structures (30) and (31), W_e and W_u for the steering and diving modes are respectively obtained as

$$W_{e\_S}(s) = \frac{0.0009561\, s + 0.07188}{s + 28.2173}, \tag{36}$$

$$W_{u\_S}(s) = \frac{s + 0.2888}{2.0880\, s + 127.9018} \tag{37}$$

and

$$W_{e\_D}(s) = \frac{0.0000012\, s + 0.0048}{s + 13.5061}, \tag{38}$$

$$W_{u\_D}(s) = \frac{s + 3.2276}{3.4831\, s + 680.0174} \tag{39}$$

4.1.2 Controller Order Reduction

Using *hinfsyn* function in MATLAB Robust Control Toolbox the H_∞ controller K_{inf} in Fig. 5 is

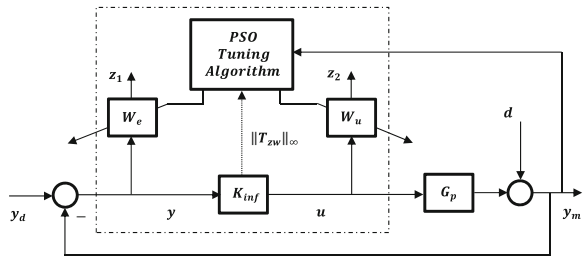

Fig. 8 The proposed block diagram for PSO-based H_∞ controller design

designed with the resulting values of γ reported in Table 5. The H_∞ controller transfer function, respectively for the steering and diving modes, are

$$K_{inf\_S}(s) = \frac{-0.1952\,s^5 - 18.23\,s^4 - 406.4\,s^3 - 1372\,s^2 - 917.7\,s - 123.9}{s^6 + 80.56\,s^5 + 1728\,s^4 + 7370\,s^3 + 7780\,s^2 + 3278\,s + 486.7} \tag{40}$$

and

$$K_{inf\_D}(s) = \frac{0.4927\,s^5 + 104.4\,s^4 + 1634\,s^3 + 4453\,s^2 + 3006\,s + 193.7}{s^6 + 194.5\,s^5 + 3467\,s^4 + 15500\,s^3 + 23950\,s^2 + 17680\,s + 6517} \tag{41}$$

Although the H_∞ synthesis is an efficient control tool to achieve robust stability and performance, but the high order of the resulting controller may be a drawback in practical implementation. Thus, the Hankel norm approximation [21], as a controller order reduction technique is applied here to the resulting controllers. The Hankel singular values for the steering and diving modes respectively obtained as

$$SV_{\_S} = [\,0.1681\,,\ 0.0426\,,\ 0.0031\,,\ 0.00080648\,,\ 0.00042460\,,\ 0.0000000010239\,]$$

and

$$SV_{\_D} = [\,0.1478\,,\ 0.1456\,,\ 0.0122\,,\ 0.00055534\,,\ 0.00014429\,,\ 0.00000000023177\,]$$

are plotted in Fig. 9.

Ignoring the small singular values the order of the steering and diving controllers are reduced to 3 and 4 respectively, with the transfer functions

$$K_{\substack{\inf \\ Sreduced}}(s) = \frac{-0.2386\,s^2 - 0.5183\,s - 0.1029}{s^3 + 3.051\,s^2 + 1.826\,s + 0.4003} \tag{42}$$

$$K_{\substack{\inf \\ Dreduced}}(s) = \frac{0.5436\,s^3 + 1.234\,s^2 + 0.4554\,s + 0.02706}{s^4 + 4.722\,s^3 + 5.722\,s^2 + 3.855\,s + 0.9016} \tag{43}$$

Table 5 Final value of γ for steering and diving mode obtained based on PSO

Subsystem	γ
Steering Mode	0.7303
Diving Mode	0.9490

The maximum singular value of the resulting closed loop systems, depicted in Fig. 10a and b is less than one. Meanwhile, the illustrations in Fig. 10c and d show that the condition $\|W_e\,S\|_\infty < 1$, or equivalently the tracking performance together with disturbance rejection, has been satisfied. Avoiding actuator saturation is also guaranteed, as Fig. 10e and f show the maximum singular value of $K_{inf}S$ is less than W_u^{-1}, i.e. $\left\|W_u K_{inf}\,S\right\|_\infty < 1$.

4.2 PSO-Based Adaptive Sliding Mode Controller

Removing some drawbacks of the H_∞ control synthesis, a systematic adaptive sliding mode controller, optimized by PSO, is proposed here to motion control of an AUV. An adaptation mechanism, without high frequency switching, is developed to deal with the system uncertainties with unknown bounds.

The both steering and diving subsystems can be described by

$$\dot{x}\,(t) = A\,x\,(t) + B\,u\,(t) + f\,(t, x) \tag{44}$$

where $x\,(t)$ is the state vector, $u\,(t)$ is the control input and $f\,(t, x)$ stands for external disturbances, unmodelled dynamics and coupling effects.

As the first step in developing the proposed ASMC scheme, define the sliding surface as

$$\sigma = S^T\tilde{x} = \begin{bmatrix} s_1 & \cdots & s_n \end{bmatrix} \begin{bmatrix} x_1 - x_{1d} \\ \vdots \\ x_n - x_{nd} \end{bmatrix} \tag{45}$$

where S represents the sliding coefficient vector and $\tilde{x} = x - x_d$ is the tracking error vector, with the desired state trajectory x_d. The control objective is to design $u(t)$ such that $\tilde{x} \to 0$, as $t \to \infty$. To this end, it is sufficient to construct a $u(t)$ with the switching gain

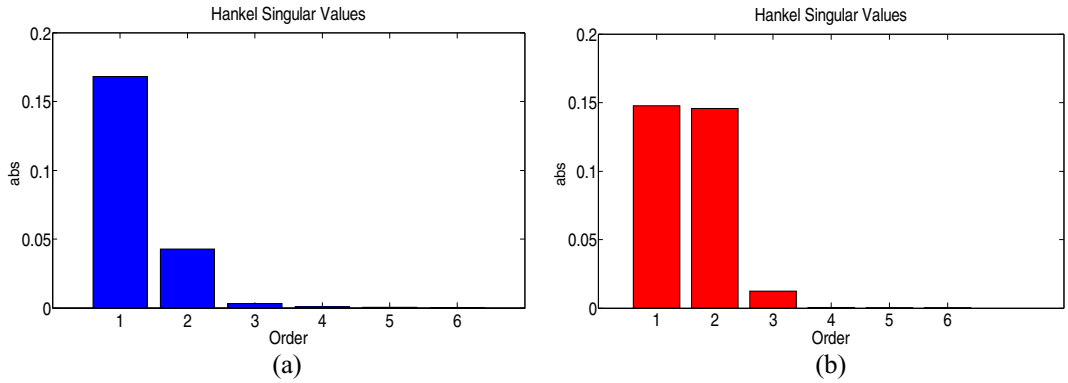

Fig. 9 Hankel singular values for (**a**) steering mode, (**b**) diving mode

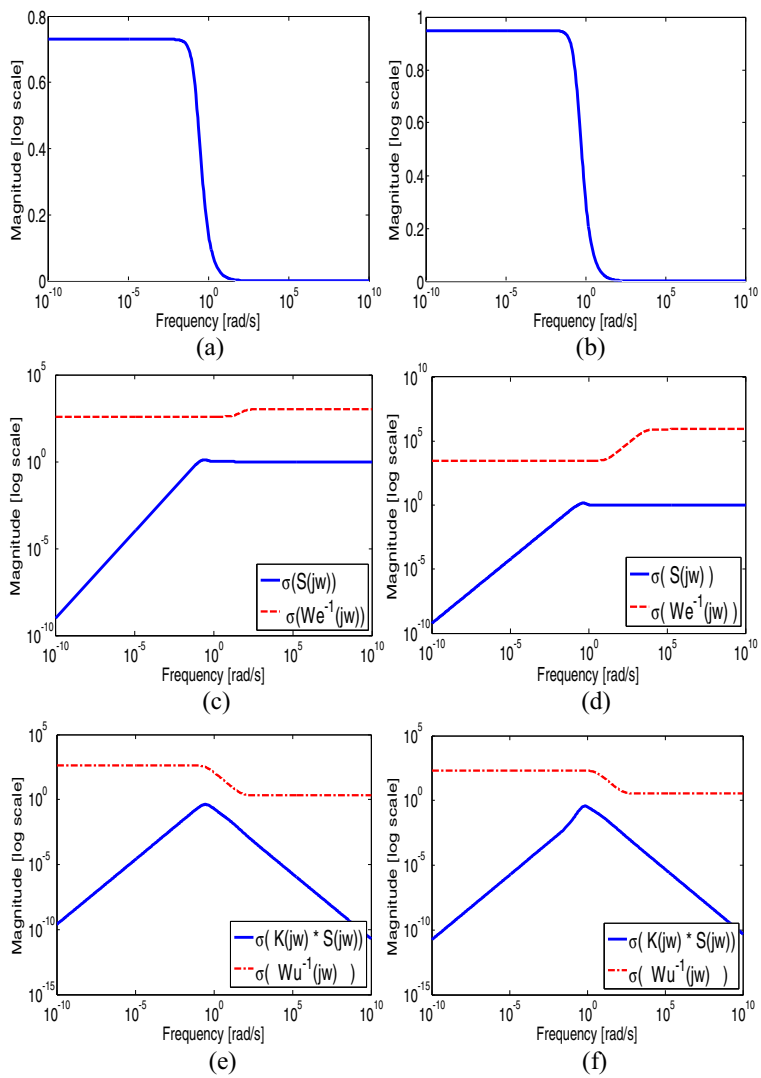

Fig. 10 Frequency characteristics, including the largest singular values of (**a**&**b**) the closed loop system, (**c**&**d**) the sensitivity function S and W_e^{-1}, and (**e**&**f**) the functions $K_{inf}\,S$ and W_u^{-1}, respectively for the steering and diving modes

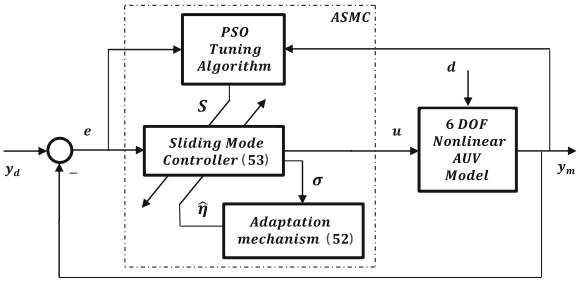

Fig. 11 Block diagram of ASMC, tuned by PSO

$\eta > 0$ which satisfies $\dot{\sigma} = -\eta\, sign\,(\sigma)$ or equivalently, $\sigma\,\dot{\sigma} < 0$. By defining $\Delta f = f - \hat{f}$, where $\hat{f}$ denotes the nominal part, it can be shown that

$$\eta > \left\| S^T \right\| . \left\| \Delta f\,(x) \right\| \tag{46}$$

ensures the robust stability. Although choosing η may be feasible by using the known upper bound of perturbations, but in the case of underwater vehicles, the complexity and unpredictably of the structure of uncertainties make such selection be difficult. To overcome such problem, an adaptation law may be derived for updating $\hat{\eta}$, as the estimate of η, to construct an ASMC.

Choosing the Lyapunov function candidate

$$V\,(\sigma, \tilde{\eta}) = \frac{1}{2}\sigma^2 + \frac{1}{2\,\gamma_\eta}\tilde{\eta}^2, \qquad \gamma_\eta > 0 \tag{47}$$

where $\tilde{\eta} = \hat{\eta} - \eta$, and taking the time derivative of $V\,(\sigma, \tilde{\eta})$, one obtains

$$\begin{aligned} \dot{V}\,(\sigma, \tilde{\eta}) &= \sigma\,\dot{\sigma} + \frac{1}{\gamma_\eta}\tilde{\eta}\dot{\tilde{\eta}} \\ &= \sigma\left(S^T\left(A\,x + B\,u + \hat{f} + \Delta f - \dot{x}_d\right)\right) \\ &\quad + \frac{1}{\gamma_\eta}\tilde{\eta}\dot{\hat{\eta}} \end{aligned} \tag{48}$$

Substituting the proposed ASMC law

$$\begin{aligned} u = \left(S^T B\right)^{-1}\Big[&-S^T A\,x - S^T\hat{f}\,(x) + S^T\dot{x}_d \\ &-\hat{\eta}\, sign\,(\sigma)\Big] \end{aligned} \tag{49}$$

in Eq. 48, where $S^T B$ is non-singular, yields

$$\dot{V}\,(\sigma, \tilde{\eta}) = \sigma\, S^T\,\Delta f\,(x) - \hat{\eta}\,\sigma\, sign\,(\sigma) + \frac{1}{\gamma_\eta}\tilde{\eta}\dot{\hat{\eta}} \tag{50}$$

Incorporating the inequality (46) into Eq. 50, gives

$$\dot{V} < \eta\,|\sigma| - \hat{\eta}\,|\sigma| + \frac{1}{\gamma_\eta}\tilde{\eta}\dot{\hat{\eta}} \tag{51}$$

Now, choose the adaptation mechanism

$$\dot{\hat{\eta}} = \gamma_\eta\,|\sigma| \tag{52}$$

to obtain $\dot{V} \leq 0$, which ensures the robust stability.

Remark 2 In practice, the limitations on choosing small sampling time and imperfect implementation of adaptation mechanism (52) may cause the estimated value $\hat{\eta}$ to increase without bound. On the other hand,$\hat{\eta}$ has direct impact on control law (49) and may cause instability. Hence, some modifications as leakage method or dead zone, as in this work, should be used.

Remark 3 Chattering phenomenon, due to the discontinuity of the sign function in Eq. 49, can be avoided by using a *tanh* function to form a modified ASMC law as

$$\begin{aligned} u = \left(S^T B\right)^{-1}\Big[&-S^T A\,x - S^T\hat{f}\,(x) + S^T\dot{x}_d \\ &-\hat{\eta}\, tanh\,(\sigma/\Phi)\Big] \end{aligned} \tag{53}$$

where the positive constant Φ is the boundary layer.

4.2.1 Selection of Sliding Coefficients by PSO

The performance of the closed loop system, formed by the ASMC and AUV subsystems, is highly dependent to numerical value of the sliding coefficients. By specifying a cost function as

$$f_1 = w_1\, M_P + w_2\, t_r + w_3\, t_s \tag{54}$$

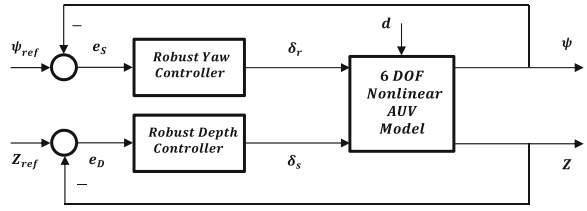

Fig. 12 The general framework of the motion control system for an AUV

Table 6 Different groups of weighting functions, obtained by using PSO

Subsystem	Weighting functions	First group	Second group	Selected group
Steering Mode	$W_{e\_S}(s)$	$\frac{0.0009032\,s+0.2109}{s+27.3001}$	$\frac{0.0007981\,s+0.05198}{s+35.2181}$	$\frac{0.0009561\,s+0.07188}{s+28.2173}$
	$W_{u\_S}(s)$	$\frac{s+0.4769}{19.1651\,s+131.6895}$	$\frac{s+0.5969}{3.5008\,s+200.8965}$	$\frac{s+0.2888}{2.0880\,s+127.9018}$
Diving Mode	$W_{e\_D}(s)$	$\frac{0.000073\,s+0.0089}{s+10.9501}$	$\frac{0.0000091\,s+0.0018}{s+16.7611}$	$\frac{0.0000012\,s+0.0048}{s+13.5061}$
	$W_{u\_D}(s)$	$\frac{s+1.9905}{5.9569\,s+506.1009}$	$\frac{s+9.0006}{2.8968\,s+845.2013}$	$\frac{s+3.2276}{3.4831\,s+680.0174}$

where w_i, $i = 1, 2, 3$, denotes some weight constants and M_P, t_r and t_s are respectively the maximum overshoot, rise time and settling time, the PSO algorithm may be adopted to optimally determine S. On the other hand, for minimizing the accumulated absolute tracking error, a cost function as

$$f_2 = \int_{t=0}^{T_f} |\tilde{x}\,(t)|\; dt \tag{55}$$

with $T_f > 0$, can be incorporated in the total objective function $f_{Total} = f_1 + f_2$ The overall block diagram of the proposed ASMC, tuned by PSO, is shown in Fig. 11.

Remark 4 Weighting function selection may be one the main problems in developing an H_∞ control algorithm [21]. There is no general structure for weighting functions, but the trial and error procedure and fine-tuning based on the time response of the system have been used before [30, 32]. In general, such strategies cannot ensure the fast response and stability properties simultaneously, whereas by defining an appropriate cost function and applying the PSO algorithm the robust stability and performance, as well as fast tracking response with disturbance attenuation are achieved here.

Remark 5 The sliding mode controllers for AUVs, developed in some previous works [33–36] has some disadvantages as

i. The upper bound of system uncertainties are assumed to be known
ii. The switching gain η is determined by trial and error.
iii. Assigning the coefficients of the sliding surface may be time consuming by the conventional

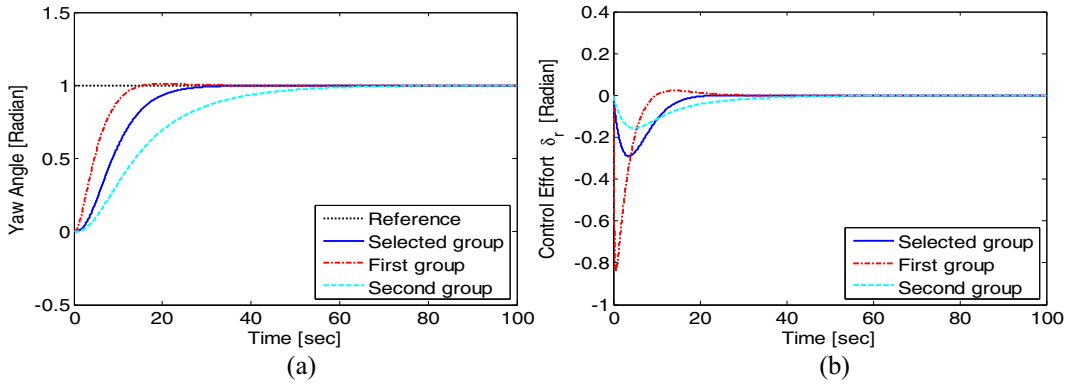

Fig. 13 Simulation results of yaw control, by applying the identification-based H_∞ controller, with various weighting functions in Table 6, (**a**) Output response, (**b**) Control effort δ_r

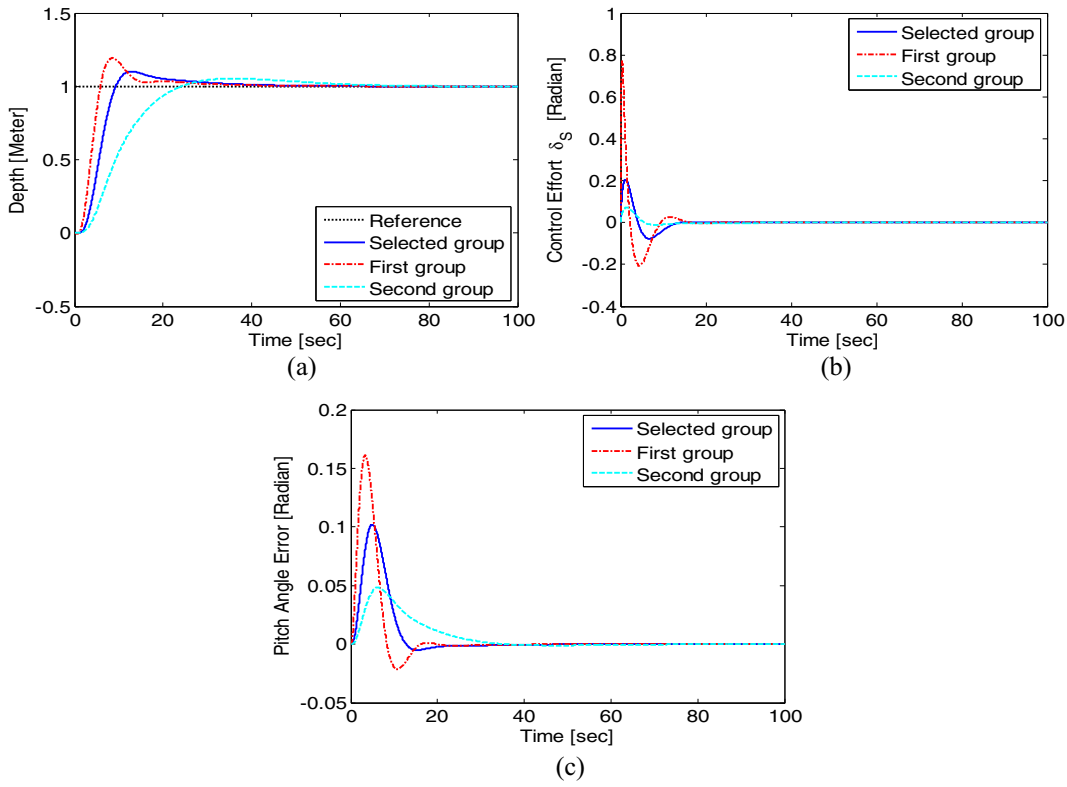

Fig. 14 Simulation results of depth control, by applying the identification-based H_∞ controller, with various weighting functions in Table 6, (**a**) Output response, (**b**) Control input δ_S, (**c**) Pitch angle error

techniques such as the geometric approach and search-based methods.

On the contrary, this paper removes the aforementioned drawbacks by the proposed ASMC, in which an adaptation law is derived for estimating η.

5 Simulation Results

The effectiveness of the developed identification-based robust motion control is evaluated here via various simulations, with adopting a 6DOF nonlinear model of the AUV, introduced by Healey et al. [22].

Table 7 The results of the PSO-based H_∞ controller by using different groups of weighting functions in $t \in [0 \quad 100^{sec}]$

Subsystem	Specification Groups	$M_P\%$	$t_r\ (sec)$	$t_{s5\%}\ (sec)$	$\|\tilde{x}\|_2$	$\|u\|_2$	Controller order	γ
Steering Mode	First group	1.15	8.56	11.86	18.63	12.21	6	0.7304
	Second group	0	29.19	43.15	32.71	4.88	6	0.7303
	Selected group	0	14.55	21.53	25.92	7.20	6	0.7303
Diving Mode	First group	19.22	3.32	13.71	17.74	7.81	6	0.9491
	Second group	5.4	14.26	41.07	27.3	1.18	6	0.9490
	Selected group	9.9	5.21	20.72	21.34	3.21	6	0.9490

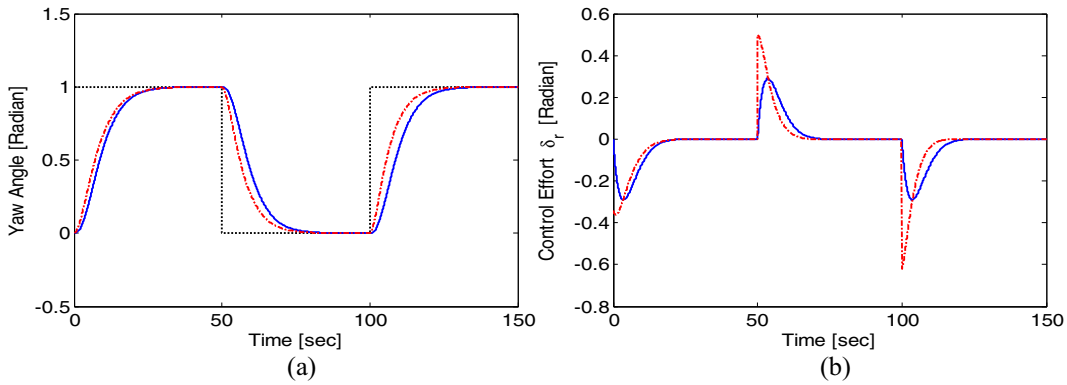

Fig. 15 Simulation results of yaw control, by applying the identification-based H_∞ controlle (–) and ASMC (– • –), (**a**) Step response, (**b**) Control effort δ_r

The physical shape of the selected AUV, called NPS AUV II is shown in Fig. 1. More details about the 6-DOF nonlinear dynamics of the model including the main properties of hydrodynamic coefficients together with the numerical values of the parameters, omitted here due to the space limitations, are completely given in [14, 22].

The initial conditions $[x_0, y_0, z_0, \varphi_0, \theta_0, \psi_0] = [0\,\text{m}, 0\,\text{m}, 0\,\text{m}, 0\,\text{rad/s}, 0\,\text{rad/s}, 0\,\text{rad/s}]$ and $[u_0, p_0, q_0, r_0] = [1.832\,\text{m/s}, 0\,\text{rad/s}, 0\,\text{rad/s}, 0\,\text{rad/s}]$, and

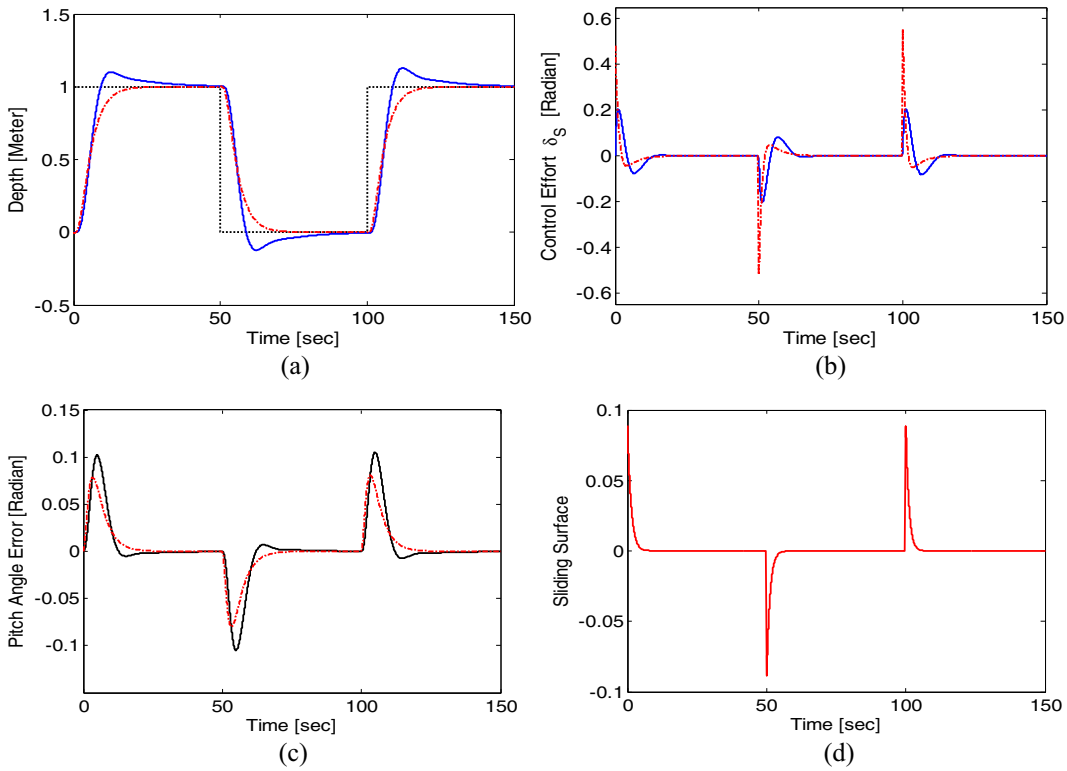

Fig. 16 Depth control by applying the identification-based H_∞ controlle (–) and ASMC (– • –), (**a**) Step response, (**b**) Control effort δ_S, (**c**) Pitch angle error, (**d**) Time history of sliding surface σ

Table 8 Final values of $\hat{\eta}$ and S for the steering and diving control, obtained by PSO in $t \in [0 \quad 50^{sec}]$

Parameters		$\hat{\eta}$	$S = [\, s_1 \;\; s_2 \;\; s_3 \,]^{\mathbf{T}}$
Optimal values	Steering Mode	1.1780	[-0.0418,0.9643,0.2614]$^{\mathrm{T}}$
	Diving Mode	0.7593	[-0.6212,-0.7786,0.0888]$^{\mathrm{T}}$

the propeller shaft speed $n = 1500$ rpm, regarding the AUV model are selected in simulation studies The general framework of the control system, formed by the nonlinear model and the proposed robust controllers in the steering and diving modes, is presented in Fig. 12.

The simulation results are presented in the following cases to evaluate the tracking performance and disturbance rejection.

Case 1 In this case, the performance of the proposed PSO-based H_∞ controller is evaluated with adopting different groups of weighting functions. In Table 6, two different groups of weighting factors (functions) are chosen to compare with the selected group (in Section 4.1.1 in Eqs. 36–39), obtained by PSO algorithm. It is important to note that, weighting functions, obtained by using PSO, satisfy the conditions $|W_e(j\omega)|^{-1} \geq |S(j\omega)|$, $\forall\omega$, and $|W_u(j\omega)|^{-1} \geq \left|K_{inf}(j\omega)\, S(j\omega)\right|$, $\forall\omega$, the same as Fig. 10.

Taking the desired state trajectory as $x_d^T = [0, 0, 1]$, in both the steering and diving modes, the time responses of the systemare illustrated in Figs. 13 and 14. From a comparison viewpoint, the time response specifications of the designed identification-based H_∞ robust motion controller, are summarized in Table 7 with $T_f = 100^{sec}$. Such comparison can be made in the sense of 2-norm of tracking error, 2-norm of control effort, and transient time specifications. The resulting values γ and the order of H_∞ controllers are similar in all three groups, whereas, the desired performance in the sense of less overshoot (M_P), faster time response (t_r), and less tracking error ($\tilde{x}$),is obtained by using the selected groups for W_e and W_u, in both the steering and diving modes.

Case 2 Taking a square command as the desired state trajectory, to show the effect of abrupt changes in positive and negative directions in both the steering and diving modes, the time responsesare illustrated in Figs. 15 and 16, in the absence of external disturbances.

The objective function for applying the PSO algorithm in ASMC is specified by choosing the weight factors $w_1 = w_2 = 50$ and $w_3 = 20$. The optimal final value of $\hat{\eta}$ and S for the steering and diving control are reported in Table 8 with $T_f = 50^{sec}$. The simulation results confirm the tracking performance by the both proposed methods, with limited control efforts. Although it is found by Figs. 15a and 16a that the reference trajectory is tracked with quite small errors by both the PSO-base H_∞ controller and the PSO-based ASMC, but Figs. 15b and 16b, show that a smaller control effort is obtained for theH_∞ algorithm.

From a comparison viewpoint, the time response specifications of the designed identification-based robust motion controllers are summarized in Table 9 with $T_f = 50^{sec}$. One can conclude that the PSO-based

Table 9 Comparison of the PSO-based H_∞ controller and ASMC in $t \in [0 \quad 50^{sec}]$

Subsystem	Specification Control algorithm	$M_P\%$	$t_r(sec)$	$t_{s5\%}(sec)$	$\|\tilde{x}\|_2$	$\|u\|_2$	$\|u\|_\infty$
Steering Mode	H_∞	0	14.55	21.53	25.92	7.20	0.28
	ASMC	0	14.45	20.52	23.11	7.90	0.36
Diving Mode	H_∞	9.9	5.21	20.72	21.34	3.21	0.20
	ASMC	0	9.22	14.33	20.76	3.48	0.48

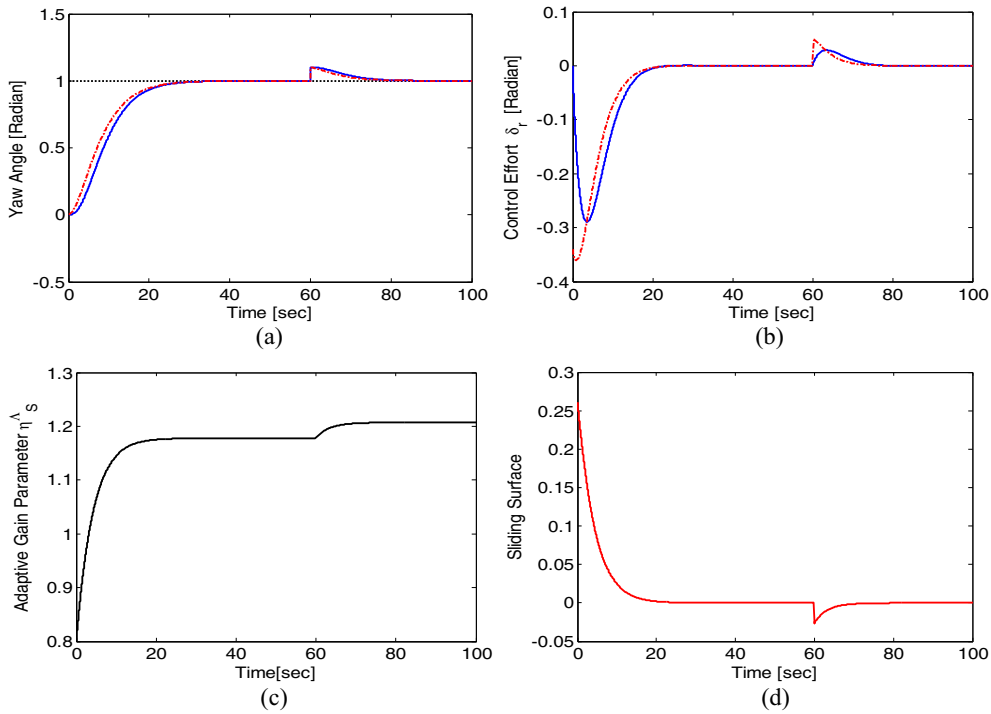

Fig. 17 Heading control by identification-based H_∞ controlle (−) and ASMC (− • −) in the presence of external disturbance $d_1\,(t)$. (**a**) Step response, (**b**) Control effort δ_r, (**c**) Adaptive gain parameter $\hat{\eta}_{\_S}$ in ASMC, (**d**) Time history of sliding surface σ

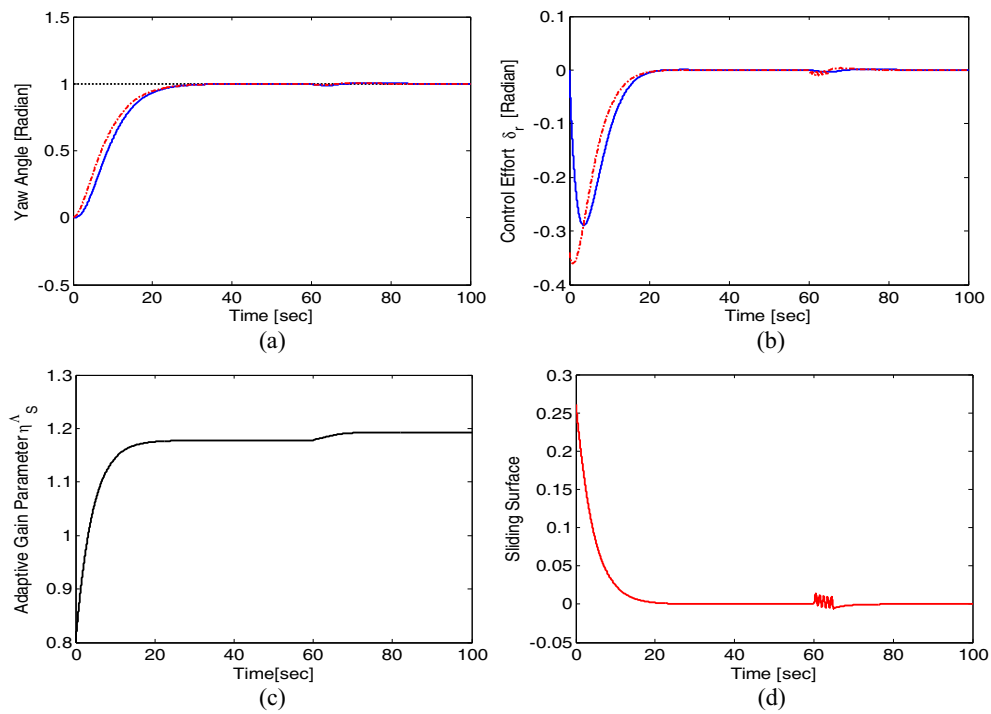

Fig. 18 Heading control by identification-based H_∞ control (−) and ASMC (− • −) in the presence of sine disturbance $d_2\,(t)$. (**a**) Step response, (**b**) Control effort δ_r, (**c**) Adaptive gain parameter $\hat{\eta}_{\_S}$ in ASMC, (**d**) Sliding surface σ

ASMC gives a better performance in the sense of less overshoot (M_P), faster time response (t_r) and less tracking error ($\tilde{x}$) and settling time (t_s). On the contrary, the PSO-based H_∞ controller presents a lower control effort (u), which facilitates controlling the vehicle to track the desired trajectory.

Case 3 In order to study the robustness properties of the designed robust controllers, consider a situation in which the external disturbance $d(t)$ perturbs the system. The performance is evaluated here against the abrupt and periodic disturbances by choosing two general structures as

$$d_1(t) = \begin{cases} 0.1 & t \geq 60\,s \\ 0 & t < 60\,s \end{cases} \tag{56}$$

and

$$d_2(t) = \begin{cases} 0.3\,sin2\pi t & 60\,s \leq t \leq 65\,s \\ 0 & otherwise \end{cases} \tag{57}$$

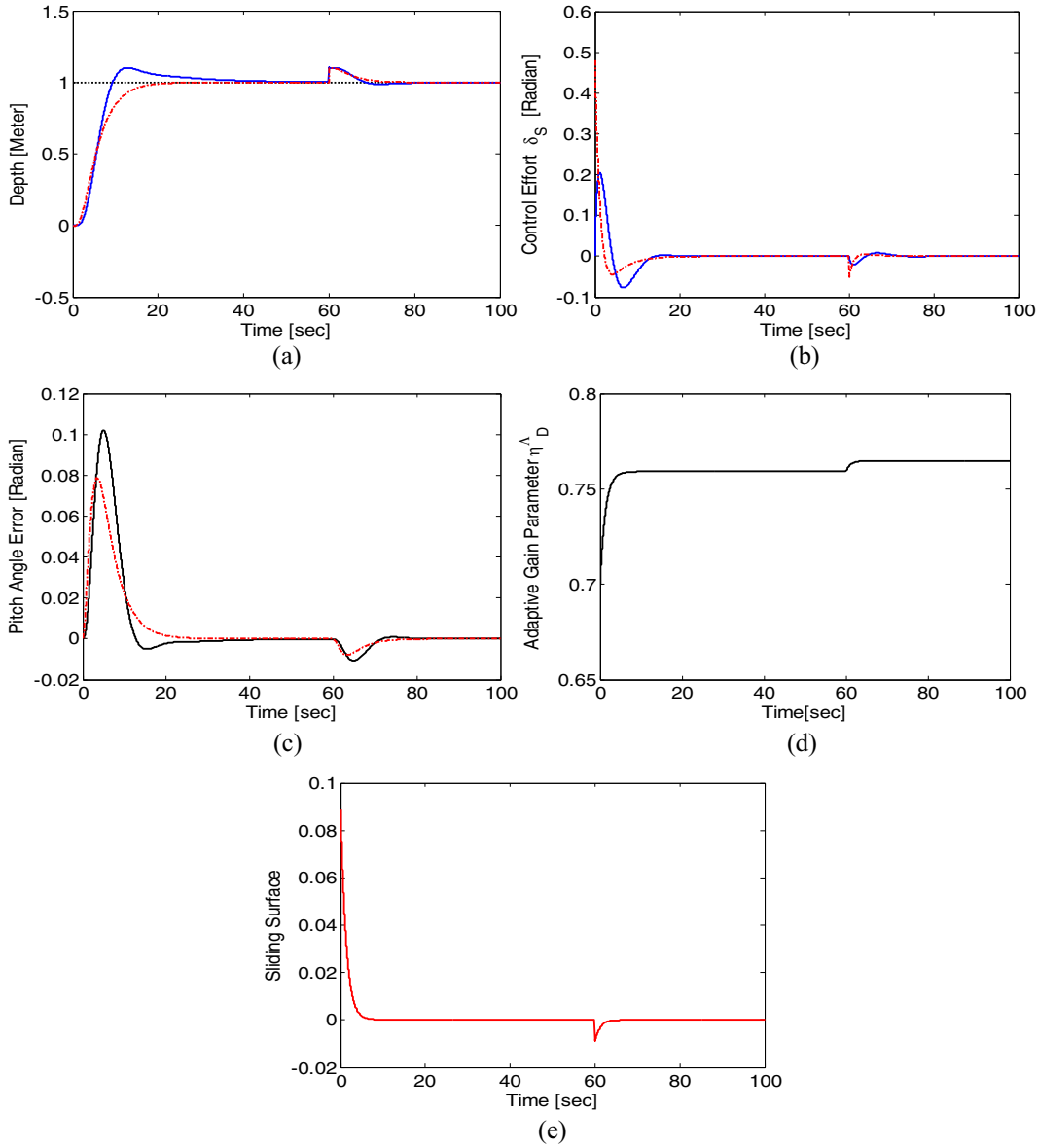

Fig. 19 Depth control by identification-based H_∞ algorithm (−) and ASMC (− • −) in the presence of external disturbance $d_1(t)$. (**a**) Step response, (**b**) Control effort δ_S, (**c**) Pitch angle error, (**d**) Adaptive gain parameter $\hat{\eta}_D$, (**e**) sliding surface σ

Taking the desired state trajectory as $x_d^T = [0, 0, 1]$, the proposed identification-based robust controllers, applied to the perturbed steering and diving subsystems, provide robust tracking performance with disturbance rejection, as demonstrated in Figs. 17 and 18 for heading control, and in Figs. 19 and 20 for diving control. The simulation results show that despite applying the external disturbance $d(t)$ to six-DOF nonlinear NPS AUV II model, the output regulation is achieved after a short time with disturbances attenuation. Furthermore, the convergence of $\hat{\eta}_{\_S}$ and $\hat{\eta}_{\_D}$ which estimate the upper bound of system perturbations is obtained. The time history of sliding surface σ in ASMC, guarantees the convergence of tracking error, i.e., $\tilde{x} \to 0$ as $t \to \infty$.

In the presence of sine disturbance $d_2(t)$, a small oscillation is made in ASMC as depicted in Figs. 18b and 20b, and also in the sliding surface σ, as reported in Figs. 18d and 20e.

Briefly discussing, regulation of the desired depth and the desired yaw angle are satisfied despite the

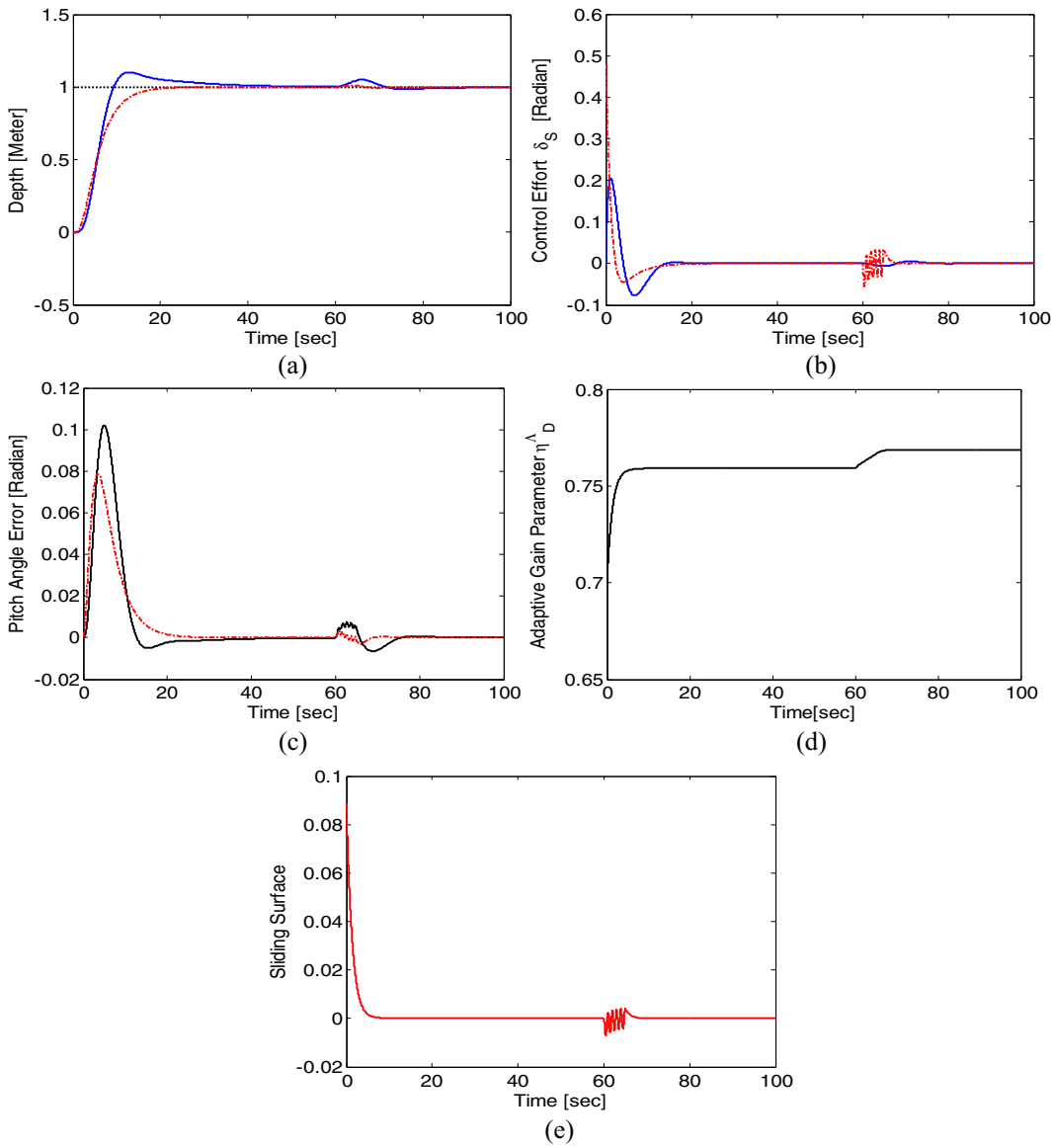

Fig. 20 Depth control by identification-based H_∞ algorithm (−) and ASMC (− • −) in the presence of sine disturbance $d_2(t)$. (**a**) Step response, (**b**) Control effort δ_S, (**c**) Pitch angle error, (**d**) Adaptive gain parameter $\hat{\eta}_{\_D}$, (**e**) sliding surface σ

model uncertainties and external disturbances for a six DOF nonlinear NPS AUV II, by using the proposed PSO-based robust controllers.

6 Conclusions

This research investigates the problem of identification-based robust motion control of an AUV in the vertical and horizontal planes. Removing the trial and error procedure, the AUV model in the steering and diving modes is identified by using an adaptive parallel-series model. The gains are optimized by the PSO algorithm, which provides achieving the fast convergence and avoiding the windup problem simultaneously. To ensure the robust stability and performance with respect to model uncertainties and external disturbances, two robust control strategies are adopted to solve the motion control problem. An H_∞ control synthesis, as a powerful technique for disturbance attenuation, is first formulated to solve the problem. The multiplicative uncertainty is preferred in formulation of a mixed H_∞ control, to deal with the cross coupling effects between subsystems, hydrodynamic parameter variations and external disturbances. In fact, the both parametric and unstructured uncertainties are incorporated into the mathematical model for the steering and diving modes in the designing procedure. The weighting functions, which play an important role in developing an H_∞ control algorithm, are selected based on an optimization criterion by using the PSO algorithm. Then, an ASMC is developed, without the complexities of weighting function selection in H_∞ control synthesis. The upper bound of perturbation is estimated by using an adaptive tuning law derived based on the Lyapunov stability theorem. The coefficients of sliding surface are optimally determined by adopting a performance index in the PSO algorithm. Finally, the identification-based robust controllers are applied to nonlinear dynamic motion equations of NPS AUV II, as a six-DOF AUV model. Robust stability and performance are explored in the steering and diving modes, in the presence of two kinds of bounded external disturbances. Simulation results are presented and discussed in three different cases, from a comparison point of view. Removing the chattering phenomenon of the conventional SMC, the proposed PSO-based ASMC presents a better performance compared with the H_∞ controller, in improving the transient time response and disturbance attenuation, at the expense of higher control effort. Identifying the model parameters of other degrees of freedom such as surge and sway modes, taking both the state and input constraints into account, and making an experimental study may be some research topics for the future works.

References

1. Zhang, Y., Streitlien, K., Bellingham, J.G., Baggeroer, A.B.: Acoustic doppler velocimeter flow measurement from an autonomous underwater vehicle with applications to deep ocean convection. J. Atmos. Ocean. Technol. **18**(12), 2038–2051 (2001)
2. Yuh, J.: Design and control of autonomous underwater robots: A survey. Auton. Robot. **8**(1), 7–24 (2000)
3. Zhang, Y., Baggeroer, A.B., Bellingham, J.G.: Spectral-feature classification of oceanographic processes using an autonomous underwater vehicle. IEEE J. Ocean. Eng. **26**(4), 726–741 (2001)
4. Kunz, C., Murphy, C., Camilli, R., Singh, H., Bailey, J., Eustice, R., Jakuba, M., Nakamura, K., Roman, C., Sato, T., Sohn, R.A., Willis, C.: Deep sea underwater robotic exploration in the ice-covered arctic ocean with AUVs. In: IEEE International Conference on Intelligent Robots and Systems, pp. 3654–3660 (2008)
5. Koofigar, H.R.: Adaptive control of underwater vehicles with unknown model parameters and unstructured uncertainties. In: Proceedings of SICE Annual Conference, pp. 192–196 (2012)
6. Ishaque, K., Abdullah, S.S., Ayob, S.M., Salam, Z.: Modeling and identification of an open-frame underwater vehicle: The yaw motion dynamics. J. Intell. Robot. Syst. **66**(1–2), 37–56 (2012)
7. Joonyoung, K., Kihun, K., Choi, H.S., Seong, W., Lee, K.Y.: Estimation of hydrodynamic coefficients for an auv using nonlinear observers. IEEE J. Ocean. Eng. **27**(4), 830–840 (2002)
8. Juan Carlos, C.L., DecioCrisol, D.: AUV identification and robust control. In: Proceedings of the 18th International Federation of Automatic Control World Congress, vol. 18, pp. 14735–14741 (2011)
9. Smallwood, D.A., Whitcomb, L.L.: Preliminary experiments in the adaptive identification of dynamically positioned underwater robotic vehicles. In: IEEE International Conference on Intelligent Robots and Systems, vol. 4, pp. 1803–1810 (2001)
10. Ven, P.W.J.V.D., Johansen, T.A., Sørensen, A.J., Flanagan, C., Toal, D.: Neural network augmented identification of underwater vehicle models. Control. Eng. Pract. **15**(6), 715–725 (2007)
11. Bossley, K.M., Brown, M., Harris, C.J.: Neurofuzzy identification of an autonomous underwater vehicle. Int. J. Syst. Sci. **30**(9), 901–913 (1999)

12. Petrich, J., Stilwell, D.J.: Model simplification for AUV pitch-axis control design. J. Ocean. Eng. **37**(7), 638–651 (2010)
13. Ioannou, P.A., Sun, J.: Robust Adaptive Control. Dover Publications (1996)
14. Fossen, T.I.: Guidance and Control of Ocean Vehicles. Wiley (1994)
15. Naeem, W., Sutton, R., Ahmad, S.M.: LQG/LTR control of an autonomous underwater vehicle using a hybrid guidance law. In: International Federation of Automatic Control, pp. 31–36 (2003)
16. Ishaque, K., Abdullah, S.S., Ayob, S.M., Salam, Z.: Single input fuzzy logic controller for unmanned underwater vehicle. J. Intell. Robot. Syst. **59**(1), 87–100 (2010)
17. Chin, C.S., Lau, M.W.S., Low, E., Seet, G.G.L.: Robust and decoupled control system of underwater robotic vehicle for stabilization and pipeline tracking. Proc. Inst. Mech. Eng. I: J. Syst. Control Eng. **222**(4), 261–278 (2008)
18. Kuo, T.C., Huang, Y.J., Yu, H.H.: FRSMC design for the steering control and diving control of underwater vehicles. J. Mar. Sci. Technol. **17**(1), 50–59 (2009)
19. Veres, S.M., Molnar, L., Lincoln, N.K., Morice, C.P.: Autonomous vehicle control systems- a review of decision making. Proc. Inst. Mech. Eng. I: J. Syst. Control Eng. **225**(2), 155–195 (2011)
20. You, S.S., Lim, T.W., Jeong, S.K.: General path-following maneuvers for an underwater vehicle using robust control synthesis. Proc. Inst. Mech. Eng. I: J. Syst. Control Eng. **224**(8), 960–969 (2010)
21. Zhou, K., Doyle, J.C.: Essentials of Robust Control. Prentice Hall (1998)
22. Healey, A.J., Lienard, D.: Multivariable sliding mode control for autonomous diving and steering of unmanned underwater vehicles. IEEE J. Ocean. Eng. **18**(3), 327–339 (1993)
23. Geranmehr, B., Nekoo, S.R.: Nonlinear suboptimal control of fully coupled non-affine six-DOF autonomous underwater vehicle using the state-dependent Riccati equation. J. Ocean Eng. **96**, 248–257 (2015)
24. Kennedy, J.: The particle swarm: Social adaptation of knowledge. In: IEEE International Conference on Evolutionary Computation, pp. 303–308 (1997)
25. Elbeltagi, E., Hegazy, T., Grierson, D.: Comparison among five evolutionary-based optimization algorithms. J. Adv. Eng. Inf. **19**(1), 43–53 (2005)
26. Fourie, P.C., Groenwold, A.A.: The particle swarm optimization algorithm in size and shape optimization. J. Struct. Multidiscip. Optim. **23**(4), 259–267 (2002)
27. Taghirad, H.D.: Belanger, P.R.: H_∞-based robust torque control of harmonic drive systems under free- and constrained-motion applications. In: IEEE International Conference on Control Applications, vol. 2, pp. 990–994 (1998)
28. Gu, D.W., Petkov, P.H., Konstantinov, M.M. Robust Control Design with Matlab, 2nd edn. Springer -Verlag, London (2013)
29. Lundstrom, P., Skogestad, S., Wang, Z.Q.: Uncertainty weight selection for H-infinity and mu-control methods. In: Proceedings of the 30th IEEE Conference on Decision and Control, pp. 1537–1542 (1991)
30. Nag, A., Patel, S.S., Kishore, K., Akbar, S.A.: A robust H-infinity based depth control of an autonomous underwater vehicle. In: International Conference on Advanced Electronic Systems, pp. 68–73 (2013)
31. Souza, E.C.D., Maruyama, N.: μ-synthesis for unmanned underwater vehicles current disturbance rejection. J. Braz. Soc. Mech. Sci. Eng. **33**(3), 357–365 (2011)
32. Feng, Z., Allen, R.: Reduced order H_∞ control of an autonomous underwater vehicle. Control. Eng. Pract. **12**(12), 1511–1520 (2004)
33. Lee, P.M., Hong, S.W., Lim, Y.K., Lee, C.M., Jeon, B.H., Park, J.W.: Discrete-time quasi-sliding mode control of an autonomous underwater vehicle. IEEE J. Ocean. Eng. **24**(3), 388–395 (1999)
34. Rodrigues, L., Tavares, P., Prado, M.: Sliding mode control of an AUV in the diving and steering planes. In: Conference Proceedings on Prospects for the 21st Century, vol. 2, pp. 576–583 (1996)
35. Tang, Z., Zhou, J., Bian, X., Jia, H.: Simulation of optimal integral sliding mode controller for the depth control of AUV. In: IEEE International Conference on Information and Automation, pp. 2379–2383 (2010)
36. Joe, H., Kim, M., Yu, S.C.: Second-order sliding-mode controller for autonomous underwater vehicle in the presence of unknown disturbances. J. Nonlinear Dyn. **78**(1), 183–196 (2014)

Sayed Hamid Mousavian was born in 1989 in Isfahan, Iran. He received his B.Sc. degree in electronic engineering with ranking 1st among all the graduated students in electrical engineering from the Isfahan University of Applied Science and Technology (UAST), Iran, in 2011, and graduated in M.Sc. degree of control engineering from University of Isfahan, Iran, in 2015. He has worked on modelling and control of autonomous underwater vehicles, based on intelligent methods, adaptive and robust algorithms. Currently, he is working on modeling and control of underwater vehicles with robust nonlinear techniques, taking the state and input constraints into account. His research interests include modelling and control of autonomous underwater vehicles, linear/nonlinear system identification, robust adaptive control, robotics, and optimization algorithms.

Hamid Reza Koofigar received the M.S. degree in Control Engineering in 2005 and his Ph.D. in Electrical Engineering in 2009, both from Isfahan University of Technology, Iran. He is with the Department of Electrical Engineering, University of Isfahan, as an associate professor, directing several industrial projects and theses in the fields of modelling and control for photovoltaic systems, hybrid systems and robotics. His current research interests include theory and applications of robust control, adaptive nonlinear control, switched systems, and renewable energy systems.